PHASE COMPOSITION OF THE CAST Co–Cr–Mo SUPER ALLOY USED IN PROSTHESES

Stoyan Parshorov* and Ivan Parshorov

Institute of Metal Science, Equipment and Technologies with Hydro- and Aerodynamics Centre "Acad. A. Balevski", Bulgarian Academy of Sciences, 67, "Shipchenski prohod" Blvd, 1574 Sofia, Bulgaria, e-mail: st.parshorov@gmail.com; parsh@ims.bas.bg

Abstract. Object of investigation is cast nickel-free Co-Cr-Mo super alloy. Data for the structure and the phase composition is obtained during different technological regime. The technological features of the alloy related to the presence of transformation induced plasticity effects and the formation of protective coatings are demonstrated.

Keywords: cobalt super alloy, prosthesis, structure, phase composition, high temperature treatment, transformation induced plasticity effects, X-ray analysis.

1. INTRODUCTION

The cobalt-base nickel free alloys used generally for manufacturing dental and surgical prostheses and implants possess a good biological tolerance and biocompatibility within the human body tissues because of the absence of nickel ions dangerous for the human health [1–6].

The implants due to their complex configuration and individuality are made mainly by means of the methods of precision casting. The application of plastic deformation to improve their properties is excluded. Therefore, the alloy has lower mechanical properties and does not use its full working and technological life.

The aim of the present paper is to study some technological features that a cast cobalt-based alloy used for medical implants offers us.

* Corresponding author.

DOI: 10.7546/EngSci.LIX.22.03.04

2. MATERIAL AND METHOD

A ten kilogram experimental casting made in a specially designed mould, in which ten sticks of different size are formed, is investigated, Fig. 1. The chemical composition of the cast alloy is given in Table 1.

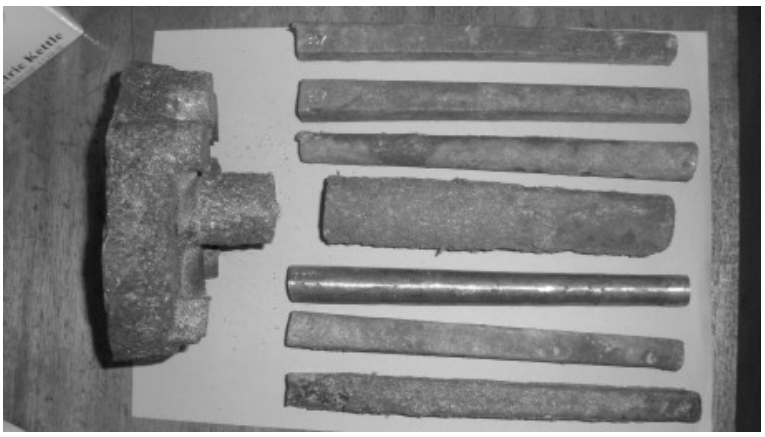

Fig. 1. Experimental mould

Table 1. Chemical composition of the investigated alloy

Cr	Mn	Fe	Ni	Mo	W	Nb	Other	Co
25.5	0.2	4.3	1.0	4.7	0.6	0.1	4.3	The rest

Table 2. Regimes of high temperature treatment

Sample No	Regime
1	Casting and homogenizing
2	Quenching at 1150 °C – 30 min, water cooling
3	Quenching at 1150 °C – 30 min, water cooling, aging at 730 °C– 4 hours, air cooling

After the casting process the ingot was homogenized at 1250 °C for 6 hours. Experimental specimens for metallographic and X-ray analysis were made by mechanical means and using electro-spark machining.

The samples are tested as cast ones and after high temperature treatment. The regimes are given in Table 2.

Macro- and micro-metallographic analysis of test specimens was performed according to standard methods. The micro-hardness is determined according

to Vickers method by means of device Micro-Duromat 4000 with load 50 g, time for reaching the load 10 s and time for acting 10 s. The micro-hardness is evaluated as average from 10 values for each phase.

The diffraction spectra for a wide interval of angles ($2 \times \theta^\circ = 15^\circ - 125^\circ$) are taken for these specimen. The X-ray structure analysis is performed by standard apparatus "Philips" with Co-K_α emission, using the following regime: step – 0.02 °/min and rate – 20 sec/step.

X-ray structural analysis of samples was performed after mechanical treatment of their surface by abrasive cleaning and subsequent polishing.

3. EXPERIMENTAL RESULTS AND DISCUSSION

3.1. Metallographic analysis

Macro-structural metallographic analysis shows a rough non-homogeneous dendritic structure with non-metallic inclusions, Fig. 2 (a, b). These features predetermined low mechanical properties and expected not high durability of the biological implant.

The microstructure study of cast alloy sample 1 shows that the mean grain size is about 220 μm, Fig. 3(a–c), and presence mainly of the low temperature ε-phase of Co, which micro-hardness HV 0.05 is 250–260 kg/mm^2, Fig. 4(a). Relatively fine precipitates of second phase are observed in the grains. They decorate some crystallographic directions of the matrix phase. This phase has a micro-hardness HV 310–345 higher than that of the metal matrix. It was determined as σ-phase – $Co_xCr_yMo_z$, according to the state diagram Fig. 5 and the results of the X-ray diffraction analysis Fig. 6.

There are precipitates observed on the grain boundaries which according to the phase diagram and the X-ray investigations show presence of the chemical compound – σ-phase ($Co_xCr_yMo_z$), Fig. 3. The precipitates are formed in the metal casting process. Non-metallic inclusions are observed Fig. 3(b, d), but no casting defects such as pores, pores and cracks are observed.

The measured micro-hardness in the field of non-metallic inclusions reaches HV 580. The average results of the Vickers hardness measurement of five test bodies are shown in Table 3, Fig. 4(a, b).

Table 3. The average results of the Vickers hardness measurement

Measurement No	1	2	3	4	5	Average
HV5	252	241	274	277	232	255
HV10	272	254	260	254	266	261

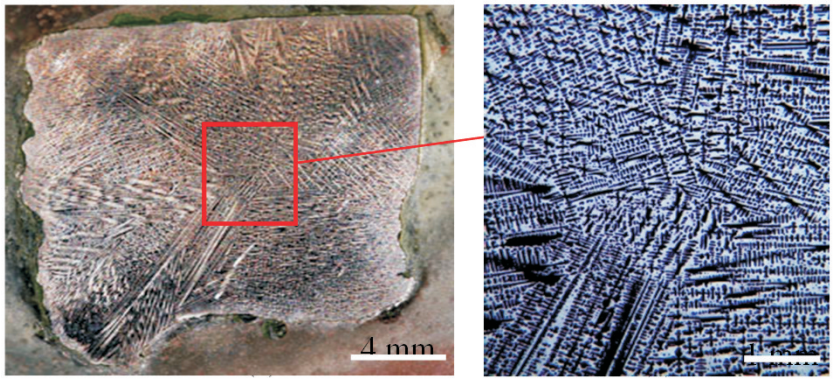

(a) (b)

Fig. 2. Macrostructure of samples of the cast stick: (a) ×2; (b) ×10

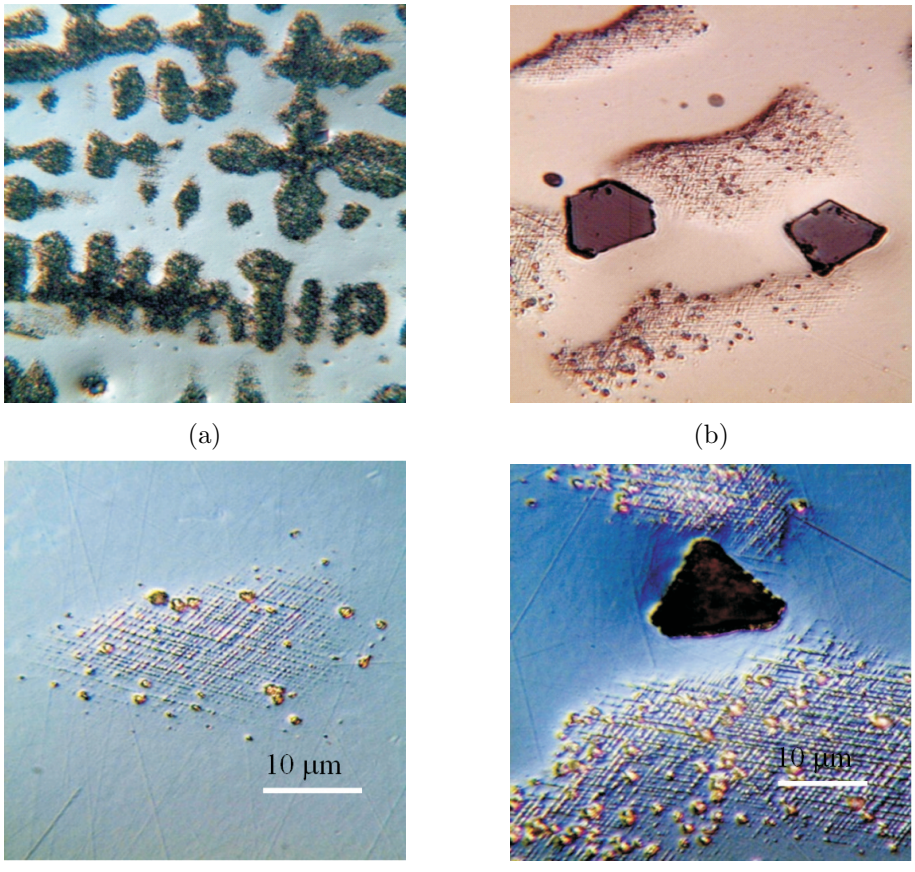

(a) (b)

(c) (d)

Fig. 3. Microstructure of the control sample: (a) ×125; (b) ×500; (c, d) ×1000

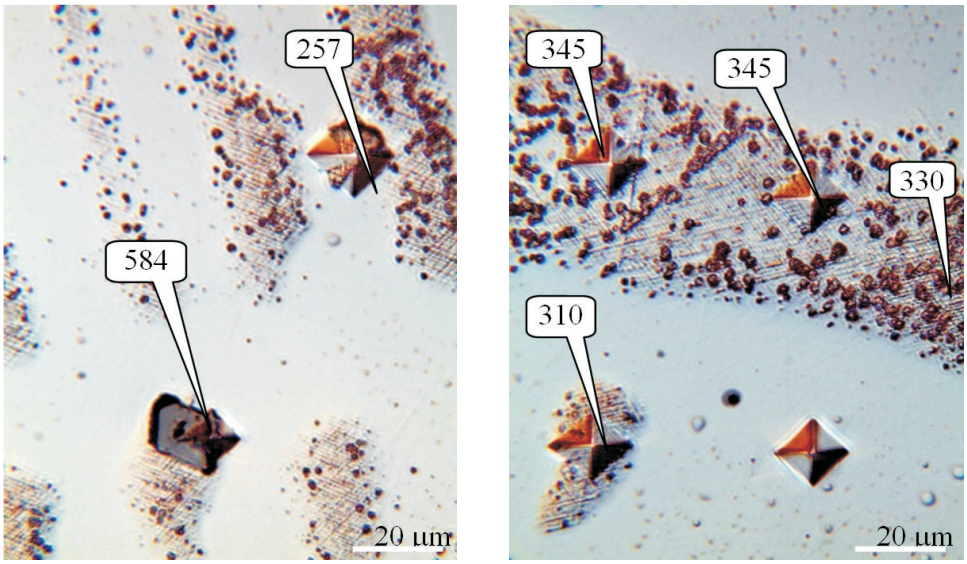

(a) (b)

Fig. 4. Micro-hardness (HV 0.05) in the cross-section of the control sample: (a, b) ×500

3.2. Technological schemes for the production of products by plastic deformation and casting

The technological parameters and conditions for preparation of the open alloy are isothermal ones and therefore these state diagrams are significantly distinguished from the isothermal ones, such as the same alloy [11–13] Fig. 5. Despite the expected quantitative mismatch between the two diagrams, the isothermal diagram of the state is at the heart of studying the phase composition of each alloy.

Figure 5 shows Co-Cr phase diagram of binary alloys. It is calculated with Thermo-Calc, coupled with PBIN thermodynamic database [12]. According to diagram, the following five phases are present in the cobalt-chromium binary system above 800 °C:

- Liquid phase;
- Cobalt-rich Face-Centred Cubic (FCC) phase, sc. γ-Co – the high-temperature modification;
- Cobalt-rich hexagonal close-packed phase, sc. ε-Co – the low-temperature modification;
- At lower temperatures 800 °C, sc. σ-phase is observed. It is a brittle inter-

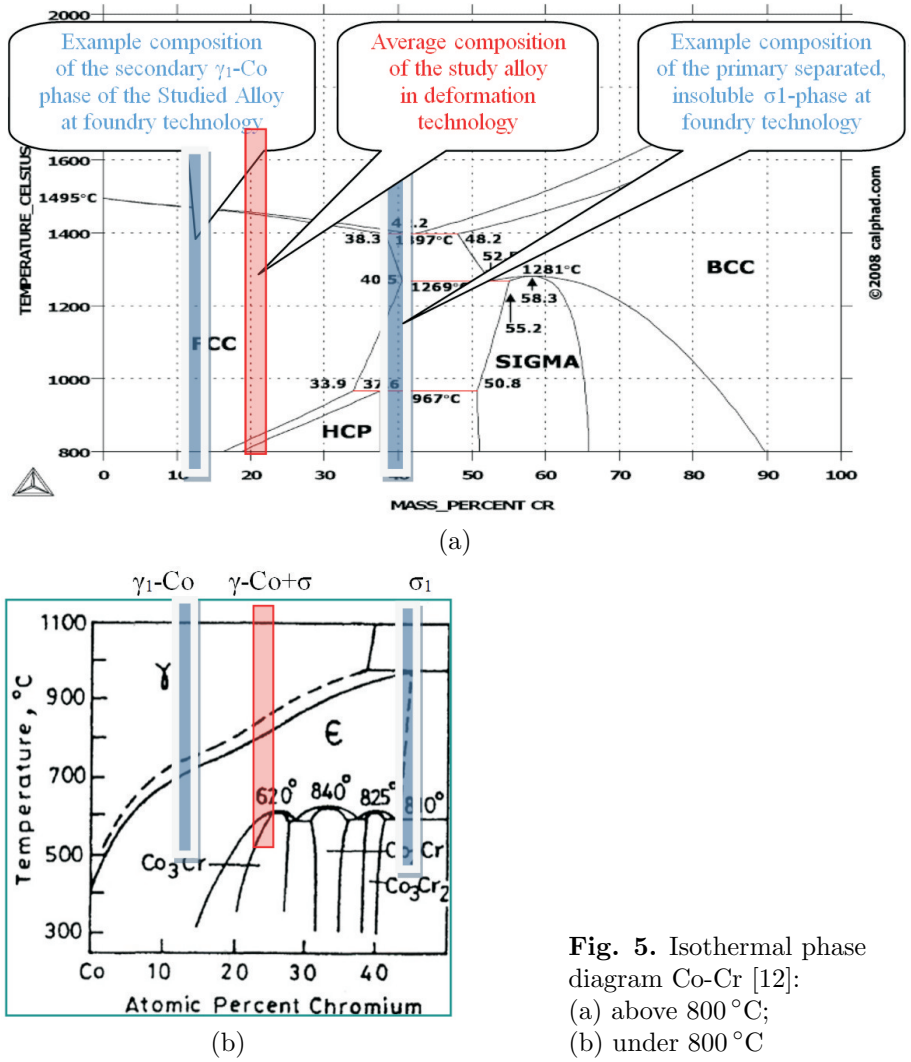

Fig. 5. Isothermal phase diagram Co-Cr [12]:
(a) above 800 °C;
(b) under 800 °C

metallic compound of cobalt and chromium with a composition corresponding approximately to the ratio Co_2Cr_3 and with the molybdenum to the $Co_xCr_yMo_z$ [12–13], Figs 3–4;

- Another phase of cobalt is chromium-rich Body-Centred Cubic (BCC) phase, sc. α-Co. It is characteristic of alloys with higher chromium concentrations and is not typical of the range of alloy tested.

There are two different basic technological schemes and phase compositions of metal products made by plastic deformation and casting.

It can be briefly formulated as follows:

- For the plastically deformed articles, the primary separated intermetallic phase is broken by deformation and during subsequent hardening it dissolves in the solid solution. After aging a secondary fine-grained intermetallic phase is separated.
- For the cast products, the primary intermetallic phase remains unchanged in the processes of heat treatment. It is only in the aging phase that a secondary fine-grained intermetallic phase is formed.

According to these technological schemes, the cast alloy does not reach its operational capabilities and its full technological and mechanical resource due to reduced mechanical properties. This fully applies to cast prostheses.

As the primary intermetallic phase is undissolved, it has a composition close to the eutectoid one for alloy, namely 42.2%, and in the cast it solidifies last, under 1379 °C (the right-blue marker) Fig. 5. In this case, the concentration of γ-Co solution is the left blue marker, under of the median in the alloy (the middle red marker).

3.3. Phase composition in heat treatment of cobalt alloy for cast implants

Figure 6 shows the X-ray diffraction spectrum of a cast sample of the test alloy. Only the diffraction lines of the high-temperature phase of cobalt, etc. are observed on it γ-Co. This shows that the other phases of cobalt ε-Co and $Co_xCr_yMo_z$, which are undoubtedly present in the alloy, cannot be identified radiographically. This is probably due to their small amounts or their high dispersion in the metal system.

The X-ray structural studies of the phase composition of the alloy are shown in Fig. 6. Based on the comparison of the maximum intensity of the diffraction maxima, it can be briefly stated [14]:

- Both cast and heat-treated samples have a composition that consists of three phases: σ-phase, γ-Co and ε-Co. The presence of the high-temperature phase is explicable, given that the amount of chromium in the alloy is significantly less than that of cobalt, and it participates in the formation of ε-Co in the peritectic reaction:

$$\gamma\text{−Co} + \sigma\text{-phase} \rightarrow \quad \varepsilon\text{-Co}.$$

- There are approximately the same amounts of σ-phase in all possible variants of casting and heat treatment, which were mentioned above.
- During hardening, a significant part of ε-Co is converted to γ-Co.

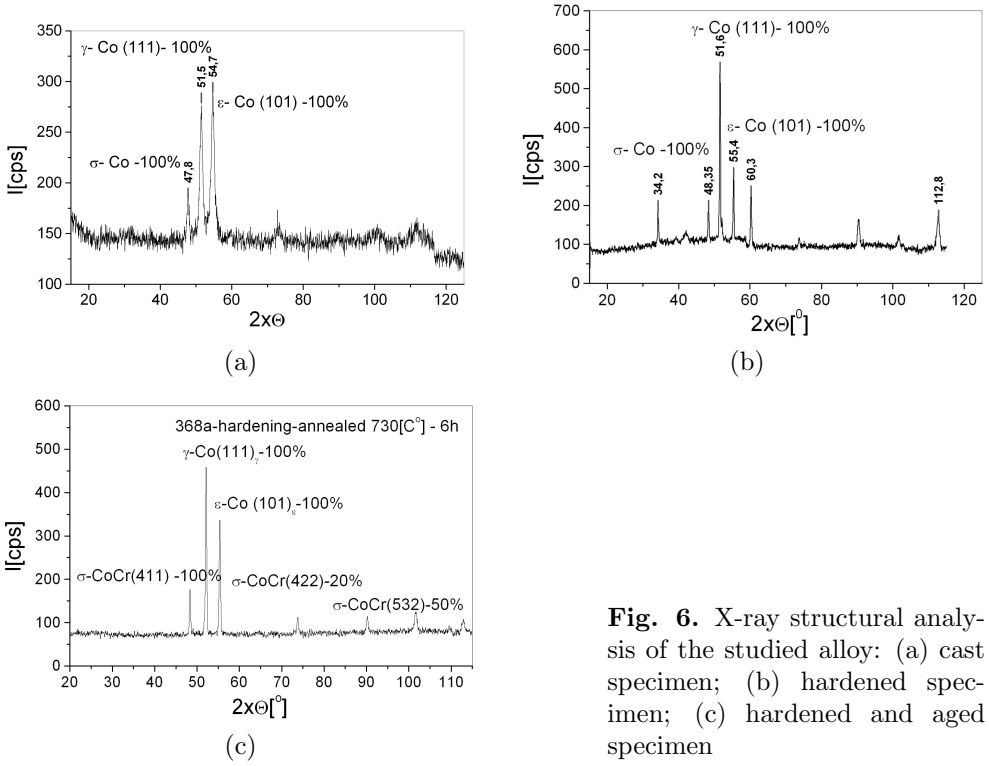

Fig. 6. X-ray structural analysis of the studied alloy: (a) cast specimen; (b) hardened specimen; (c) hardened and aged specimen

• At aging, there is an increase in the amounts of σ-phase and γ-Co, at the expense of a decrease in that of ε-Co, which can be expected to be a reversible reaction of the peritectic alloy.

3.4. Passivating cobalt oxide coatings

For the quenched specimen the X-ray diffraction analysis showed that during the heating process and holding at the quenching temperatures a thick oxide layer develops, which should be taken into account in the production of an implant. The metallographic investigations showed that the thickness of the oxide layer is 60–100 µm and it consists mainly of cobalt oxides of the type Co_3O_4.

The X-ray diffraction analysis of quenched and aged specimen again showed presence of considerably thick oxide layer with composition close to the one obtained after quenching, Fig. 7. The thickness of the oxide layer is 120–130 µm. It means that in the production process the development of the oxide layer should be taken into account. It particularly considers implants for which

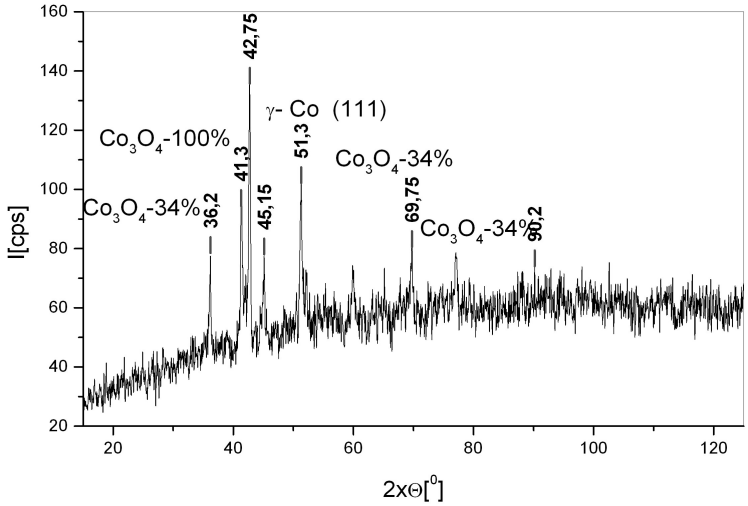

Fig. 7.. Phase composition of the surface layer after heat temperature treatment

the dimensional factor is of a great importance. The phase composition (γ-Co and ε-Co) of the alloy after the mechanical cleaning is shown in Fig. 7. In this case the two lines (111) and (200) of γ-Co are the highest ones.

3.5. TRIP effects after surface machining

After a mechanical cleaning of the surface of the specimen the diffraction lines of γ-Co and ε-Co can be seen on the roentgenogram, but the σ-phase is not presented in Fig. 8. It is unusual that the 40%-line of γ-Co-(200) is many times higher than the 100%-line of γ-Co-(111). A probable explanation of that could be that the residual stresses from the quenching have led to a "modification" of the γ-Co. To that moment there is no data in the literature to what extend the properties of the "modified" γ-Co correspond to those in "equilibrium".

A microstructural strengthening mechanism known in the literature as the TRIP effect or a mechanism described in detail in the literature by Olson and Cohen has been observed [15–16]. This feature of cobalt alloys can successfully be used for their surface hardening. Figure 8 shows the change in the phase composition of the surface of the investigated alloy under mechanical influences – grinding and polishing. There is a disappearance of the ε-Co line, i.e. a phase transformation has taken place after mechanical rather than thermal action. This subject needs an additional research.

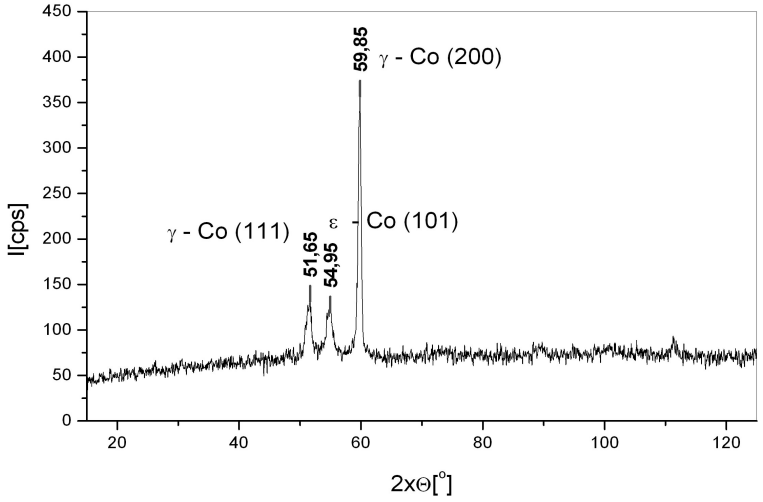

Fig. 8. Phase composition after hardening, aging and machining

Cobalt super alloys are characterized by low stacking fault energy of the solid solution, typical of solid solutions with a face-centered cubic lattice. In them the stacking fault defects are in high concentration, they are surrounded by widely split partial dislocations and in crystallographic terms they represent an ε-phase with a hexagonal lattice. In the presence of applied external load and the appearance of micro-plastic acts in the material, ε-martensite turns into a new α-phase with a body-centered cubic lattice.

4. CONCLUSION

The X-ray diffraction analysis of the phase composition of the investigated Co-Cr-Mo alloy showed:

– The phase composition of the alloy in cast form is close to the composition in the phase diagram;
– The temperature treatment of the implants – quenching and/or aging, is connected with development of a thick oxide layer which should be taken into consideration during their production process;
– After quenching and aging no σ-phase is developed in the alloy and its composition is mainly γ-Co and ε-Co;
– During the heat treatment, a dense protective oxide layer forms on the implants;

– Cobalt super alloys are characterized by high concentration of low stacking fault energy, and by applied external load ε-martensite turns into a new α-phase with a body-centered cubic lattice.

ACKNOWLEDGEMENTS

The authors are grateful to the financial support of Bulgarian National Science Fund at the Ministry of Education and Science, Contract No. DN17/17 (12.12.2017).

All equipment and experimental units used in this work was funded by the European Regional Development Fund within the OP "Science and Education for Smart Growth 2014–2020", project CoE "National center of mechatronics and clean technologies", No. BG05M2OP001-1.001-0008-C08.

REFERENCES

[1] D. Bunea, D. Bojin, S. Zamfir, F. Miculescu, and M. Miculescu, Experimental Researches Concerning the Co-Cr-Mo Alloys Used in Implantology, *European Cells and Materials* (2003) **5** (1) 53–54, ISSN: 1473-2262.

[2] M. Caicedo, R. Desai, K. McAllister, A. Reddy, J. Jacobs, and N. J. Hallab, *Journal of Orthopaedic Research* (2013) **31** (10) 1633–1642.

[3] B. Li, A. Mukasyan, and A. Varma, Combustion Synthesis of CoCrMo Orthopedic Implant Alloys: Microstructure and Properties, *Materials Research Innovation* (2003) **7** 245–252.

[4] P. Panigrahi, *Corrosion Behavior of Solution-Annealed CoCrMo*, Medical Implant Alloys Department of Materials Science and Engineering, The McCormick School of Engineering and Applied Sciences, Northwestern University (2011) **6** 32.

[5] F. George, V. Vander, E. Manilova, G. Lucas, and L. Buehler, 41 Waukegan Road, Lake Bluff, IL 60044 USA, *Metallographic Techniques for Superalloys*, http://www.georgevandervoort.com/met_papers/NickelandAlloys/met_ echs_for_superalloys.pdf. September, 2004, 19.

[6] A. Issel and L. Lim, *Biocompatibility of Stent Materials*, MURJ (2004) **11** 33–37.

[7] T. Narushima, Alfirano, S. Mineta, N. Shigenobu, Y. Takashi, and U. Kyosuke, Precipitates in Biomedical Co-Cr-Mo-C-Si-Mn Alloys, *Advanced Materials Research* (2011) **277** 51–58.

[8] O. Sahin, A. Tuncdemir, H. Cetinkara, H. Guder, and E. Sahin, Production and Mechanical Behaviour of Biomedical CoCrMo Alloy, *Chinese Physics Letters* (2011) **28** (12) 126–201.

[9] G. F. Vander Voort and G. M. Lucas, Metallography and Microstructures Heat-Resistant Alloys, *ASM Handbook*, Buehler Ltd. (2004) **9** 820–859, DOI: 10.1361/asmhba0003737.

[10] D. Sun, J. Wharton, and R. Wood, Microabrasion-Corrosion of Cast CoCrMo: Effects of Micron and Sub-micron Sized Abrasives, *Wear* (2009) **267** (1–4) 52–60, DOI: 10.1016/j.wear.2009.01.011

[11] S. Parshorov and R. Lazarova, Some Phenomena of Biomedical Cobalt-Basis Alloy, *Defectoscopy* (2012) 175–177.

[12] K. Gupta, Phase Diagram Evaluations: Section II, The Co-Cr-Mo (Cobalt Chromium-Molybdenum) System, *JPEDAV* (2005) **26** 87–92.

[13] P. Villars, A. Prince, and H. Okamoto, *Handbook of Ternary Alloy Phase Diagrams*, ASM International (1995).

[14] S. Parshorov and R. Lazarova, Phase Composition of Cast Nickel-free Superalloy, *Journal of Material Sciences and Technology* (2014) **LI** (3) 183–190.

[15] G. Olson and M. Cohen, *Journal of the Less-Common Metals* (1972) **28** 107–118.

[16] G. Olson and M. Cohen, Metal Trans (1975) **6A** 793–782.

Received February 15, 2022